Scientific
Research

An Electrochemical Nitrite Sensor Based on a Multilayer Film of Polyoxometalate

Yosra Sahraoui[1,2], Sana Chaliaa[3], Abderrazak Maaref[1], Amor Haddad[3],
Nicole Jaffrezic-Renault[2*]

[1]Laboratory of Interfaces and Advanced Materials, Faculty of Sciences of Monastir,
Monastir, Tunisia
[2]University of Lyon, Institute of Analytical Chemistry, Villeurbanne, France
[3] Laboratory of Materials and Crystallochemistry, Superior Institute of Applied Science and Technology,
Mahdia, Tunisia
Email: *nicole.jaffrezic@univ-lyon1.fr

ABSTRACT

In this work, we have developed an electrochemical sensor for nitrite detection, based on a polyoxometalate (POM) namely mono-lacunary keggin anion $[SiW_{11}O_{39}]^{8-}$ cited as (SiW_{11}). Electrochemical characterization of SiW_{11} shows two-step reduction processes, with formal potentials of -0.5 V (I) and -0.68 V (II). Oppositely charged polyelectrolyte (poly (allylamine hydrochloride) (PAH)) and (SiW_{11}) were assembled alternately to modify glassy carbon electrode. The electrochemical behavior of the modified electrode was studied in detail using cyclic voltammetry (CV). The results showed that SiW_{11}/PAH/GC electrode present good electrocatalytic activity for the reduction of nitrite. The sensor showed a dynamic range from 100 μM to 3.6 mM of nitrite and no interference from other classical anions. Experimental factors that affect electron-transfer rate in these films, such as pH effect and layers number, were systematically analyzed.

Keywords: Nitrite Sensor; Polyoxometalate; Mono-Lacunary Keggin Anion; Layer by Layer Assembly Process

1. Introduction

The presence of nitrite in groundwater and atmosphere is an essential precursor in the formation of nitrosamines, many of which have been proven to be powerful carcinogens [1-3]. The increase in nitrite concentration in the blood causes a decrease in oxygen transport by the blood causing methemoglobinemia, better known as the "blue baby syndrome" reaction of nitrite with Fe (II) forming hemoglobin to methemoglobin, HbFe (III) [4]. For these reasons, determination of nitrite has received considerable attention. Many methods have been developed for nitrite determination including spectrophotometry [5], chromatography [6] and electrochemical methods [7-12], which are advantageous over the other methods in terms of cost and time.

Electrochemical determination of nitrite ion requires a large over potential at almost all electrode surfaces [13-15]. The better way to achieve nitrite detection at low overpotentials is the use of mediators confined at the electrode surface. Over the years, numbers of modification procedures have been reported for the construction of modified electrodes [17-19]. Many studies reported the capability of hexacyanoferrate anion complex [20] for the homogeneous electrocatalytic reduction of nitrite and employed this catalytic reduction method for determination of it in real samples. They demonstrated also, that the poly-ortho-toluidine can catalyze the nitrite reduction as heterogeneous catalysis [21].

Polyoxometalates (POMs), a large family of charged, nanoscopic inorganic clusters, are attractive materials for electrode modification because of their reversible redox behavior, good chemical stability and electronic conductivity [22]. These compounds are also resistant to oxidative degradation due to the fact that their fundamental elements are in their higher oxidation state [23-26]. These properties make them very attractive in many fields such as electrochemistry, catalysis and for biomedicinal tasks [23,27-30].

There is a different type of polyoxometalates [27], and in our study Keggin-type POMs are specifically used. They

display a quite well-known structural motif that is composed of a tetrahedrally coordinated central hetero atom surrounded by four W_3O_{13} groups (triads) that are connected in a corner-sharing fashion via oxygen atoms [31, 32]. Lacunary Keggin structures $[SiW_{11}O39]^{8-}$ (SiW_{11}) used in this study, are derived from the parent Keggin type by the removal of specific WO_6 moieties, followed by an optional rotation of the remaining WO_6 octahedra [33,34]. As a consequence, (SiW_{11}) is characterized by the presence of more terminal oxygen atoms, which give them more negative charge than other POMs structure.

Layer-by-layer (LBL) self-assembly has proved to be a promising method for the fabrication of ultrathin films. It is based on the alternate adsorption on the substrate surface of oppositely charged species from dilute solutions and film formation is attributed primarily to electrostatic interaction and Van der Waals forces. It provides thickness control at the nanometer level, which can be easily adapted for automated fabrication. It is applicable to any substrate shape and also permits co-assembly with different functional components [35]. Owing to these advantages, the layer-by-layer approach has been utilized to fabricate POM-containing multilayer film consisting of synthetized or natural polyelectrolytes. Several studies used the parent Keggin silicotungstate $[\alpha-SiW_{12}O_{40}]^{4-}$ as the anion and, for example, polyaniline [36], chitosan [37] or poly (diallyldimethylammonium chloride) [38] as the counter cation source. There are only few examples of the use of lacunary Keggin polyoxotungtate anions in films prepared by the layer-by-layer self-assembly method [39]. It has been reported that metal-substituted Keggin silicotungstate could be used as mediator for the electroreduction of nitrite [40]. In this paper, we show the capability of SiW_{11} anion immobilized by electrodeposition and LBL methods, for the electrocatalytic reduction of nitrite and this property is applied for the first time for the design of a selective amperometric sensor for nitrite.

2. Experimental

2.1. Materials

Ultrapure milliQ water with a resistance of 18.2 MΩ cm was used for all experiments. P-phenylenediamine (PPD), poly (allylamine hydrochloride) (PAH) (MW 15,000), sulfuric acid (H_2SO_4), sodium nitrite ($NaNO_2$), the following product were purchased from commercial sources and used without further purification from Sigma-Aldrich. Gold nanoparticles 20 nm diameter, stabilized suspension in 0.1 M PBS were commercial products from Sigma-Aldrich. Solution of redox probe (1.0 mM) was prepared dissolving the appropriate amounts of $\left[Fe(CN)_6\right]^{3-/4-}$ in 1 M KCl.

$K_8[\alpha-SiW_{11}O_{39}]\cdot13H_2O$ was synthesized as the litera-

ture described [41]. Briefly, a solution of 4 M HCl was added over 10 min, to a mix of sodium meta-silicate solution (2.23 g, 10 mM) (Solution A), and sodium tungstate (36.29 g, 110 mM).

Solid Potassium Chloride (20 g) was then added to the solution with gentle stirring, after 15 min the precipitate was collected by filtration. Purification was achieved by dissolving the product in water (200 mL) and insoluble material being removed by filtration on a fine frit. The salt was precipitated again by addition of solid potassium chloride (10 g) before being collected by filtration, washed with 2 M potassium chloride and air dried to give $K_8[\alpha-SiW_{11}O_{39}]\cdot13H_2O$ as a white powder (13.86 g, 33.6%).

2.2. Apparatus

Electrochemical measurements were carried out using a potentiostat-galvanostat VOLTALAB 40 PGZ/301, 746 VA Trace Analyzer (Metrohm) equipped with a 747 VA Stand. A three-electrode system was used, the side arms contained Ag/AgCl (sat. KCl) reference electrode and a platinum counter electrode with a surface area of approximately 1 cm^2. The working electrode was a SiW_{11} modified glassy carbon electrode (3 mm diameter, surface area: 7 mm^2). Prior to coating, the GCE was conditioned by a polishing/cleaning procedure. The GCE was successively polished with 1.0, 0.3, and 0.05 μm α-Al_2O_3 paste and then rinsed with ultra-pure water to remove any residual alumina and finally sonicated for 5 min in an ultrasonic bath and dried under a stream of pure nitrogen.

SEM characterization of the films was performed using a Quanta ^{TM} 250 microscope (FEI) in degraded pressure mode; no gold coating was required. The infrared spectra were recorded as KBr pellets, in the 4000 - 400 cm^{-1} range on a Nicolet 470 FT-IR spectrophotometer.

Dynamic light scattering (Zetasizer Nano-ZS, Malvern Instruments) was used for the determination of the zeta potential.

2.3. Preparation of the Modified Electrodes

SiW_{11} modification of GC electrode was performed by using electrodeposition and layer-by-layer methods for the building of multilayers, by alternately dipping the desired substrate in PAH and SiW_{11} solutions, in cyclic mode [42]. **Figure 1** displays a schematic representation of the different layers of the SiW_{11}/LBL film.

The GC electrode was first placed in 2 mM PPD solution and the potential was repeatedly scanned. PPD was electropolymerized onto GCE surface by amine cation radical formation. The oxidation peak gradually diminishes and is almost absent after the 6th cycle, this observation indicates the formation of a coating on the electrode surface (cf. **Figure 2**).
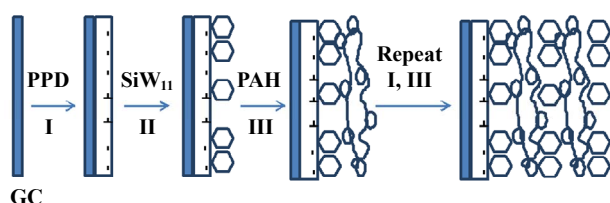
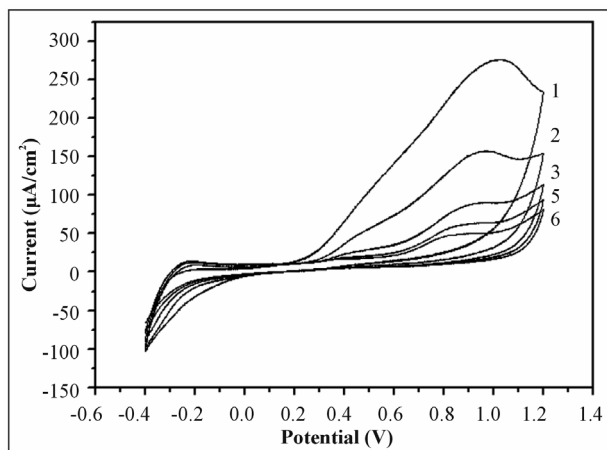**Figure 1. Schematic representation of 5-SiW₁₁/PAH/PPD/ GCE multilayer films.**

Figure 2. Cyclic voltammograms on a freshly polished GCE in 2 mM PPD solution, for the (1) first, (2) second, (3) third, (5) fifth and (6) sixth cycles, at a scan rate: 100 mV/s.

The polyPPD.GC electrode was then placed in 2 mM (SiW₁₁) solution, 0.1 M H_2SO_4 and at the same time a cyclic potential sweep was conducted in the potential range 0.8 V to −0.8 V at a scan rate of 100 mV/s⁻¹, for 25 cycles. In this way, a SiW₁₁ monolayer was deposited on the surface of polyPPD/GCE [42]. Then, the resulting electrode (SiW₁₁/polyPPD/GC) was transferred to 2 mM PAH (pH = 3) for 15 min, for resulting in one layer of positive charge. This procedure (SiW₁₁/PAH) was repeated until obtaining 5 layers of SiW₁₁.

3. Results and Discussion

3.1. Characterization of SiW₁₁ in Solution

The prepared compound was characterized by infrared spectroscopy, and cyclic voltammetry in acidic aqueous solution, because Keggin type and its derivative are unstable in neutral and basic solutions. The cyclic voltammogram becomes ill-defined and peak current much smaller, such an observation has been reported by Cheng *et al.* [43] on Keggin-type polyoxometallates. The FT-IR spectra of the lacunary keggin silicotungstate in KBr pressed pellets are presented in (**Figure 3**).

The attributions of FT-IR spectra exhibits characteristic bands at 3424.0, 1634 ν(OH); 988.4 ν_{as}(Si-O); 945.4 cm⁻¹ ν(W = O); 882.1, 733.8, 624.7 ν_{as} (W-O-W); 532.2

δ(O-Si-O) cm⁻¹. The silicotungstate vibrational spectrum was in agreement with previously reported analysis [44].

The redox behavior of SiW₁₁ in solution (conditions: 2 mM SiW₁₁ in 0.1 M H_2SO_4 solution) was studied by cyclic voltammetry and polarography. The dissolved SiW₁₁ shows that the CV curve exhibits two pairs of successive redox waves with cathodic peaks located respectively EpcI = −0.5 V (I) and EpcII = −0.68 V (II), and peak separation potentials (ΔEp) of 65 and 44 mV respectively, in the potential range from +0.8 V to −0.8 V (**Figure 4(a)**). This result is consistent with that in literature [45]. These redox waves correspond to the reduction of the tungsten centers within the SiW₁₁ ($W^{VI} \rightarrow W^{V}$). The reduction of heteropolyanions is accompanied by protonation, therefore, the pH of solution has a great effect on the electrochemical behavior of heteropolyanions.

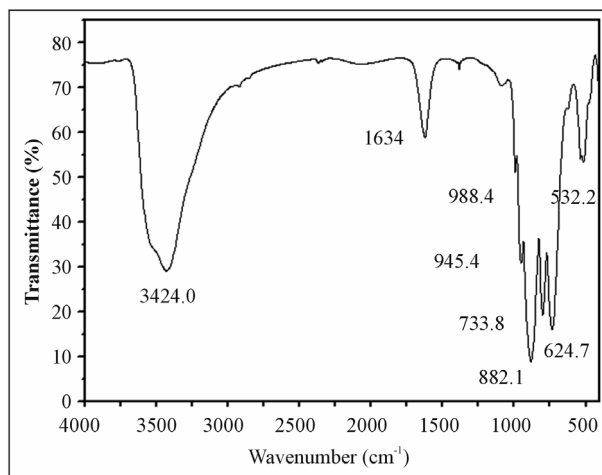The pH effect on the electrochemical behavior of the

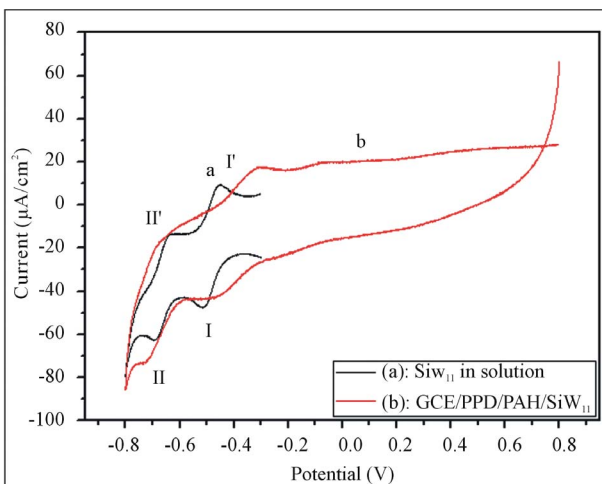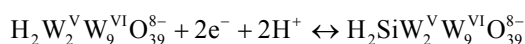**Figure 3. The FT-IR spectra of the K₈[α-SiW₁₁O₃₉]·13H₂O.**

Figure 4. Cyclic voltammograms of: (a) 2 mM SiW₁₁ in 0.1 M H₂SO₄ solution and (b) multilayer film of 5-SiW₁₁/PAH/ PPD/GCE at a scan rate: 100 mV/s.

soluble SiW_{11} was studied by polarography. The peak potentials for both redox couples shift to the more negative direction with increasing pH. Plots of Ep of the two successive redox waves (step I and step II) versus pH for the (SiW_{11}) (**Figure 1S**), show good linearity in the pH range from 0.8 to 4.3. Slopes in this pH range are −69, −85 mV pH step (I) and (II), respectively, which are close to the theoretical value of −60 mV per pH for the $2e^-/2H^+$ redox process [46]. The above results may indicate the two overall redox process of (SiW_{11}) in acidic solution as follows:

(step 1)

$$SiW_{11}^{VI}O_{39}^{8-} + 2e^- + 2H^+ \leftrightarrow H_2SiW_2^V W_9^{VI}O_{39}^{8-}$$

(step 2)

$$H_2W_2^V W_9^{VI}O_{39}^{8-} + 2e^- + 2H^+ \leftrightarrow H_2SiW_2^V W_9^{VI}O_{39}^{8-}$$

3.2. Characterization of the Modified Electrode

3.2.1. Electrochemical Characterization
Define abbreviations and acronyms the first time they are used in the text, even after they have been defined in the abstract. Abbreviations such as IEEE, SI, MKS, CGS, sc, dc, and rms do not have to be defined. Do not use abbreviations in the title or heads unless they are unavoidable.

Through the attachment of polyPPD containing NH_2 group to the GCE, the modified electrode (poly) PPD/GCE was positively charged at least up to pH 6.1 [47]. The PPD-modified GCE with an amido-terminated monolayer can be used as a charge-rich precursor to assemble oppositely charged species by layer-by-layer electrostatic interaction [48]. The adsorption of a layer of SiW_{11} is evidenced through the behavior of the modified electrode in presence of $\left[Fe(CN)_6 \right]^{3-/4-}$ redox probe (cf **Figure 5**, curves a and b). The presence of the negative layer of SiW_{11} increases ΔEp by more than 100 mV and decreases, mainly the cathodic peak, which is due to the electrostatic repulsion of the probe.

The electrostatic interaction of PAH with SiW_{11} was evidenced by using gold nanoparticles initially covered with a citrate monolayer, a layer on PAH being adsorbed on their surface, their zeta potential was found to be +44 mV. After adsorption of SiW_{11}, the zeta potential became equal to −1.1 mV, then showing the neutralization of the positive charge by successful adsorption of SiW_{11}.

Figure 5 shows that with increasing the number of SiW_{11} layers from one to five, the peak maxima of $\left[Fe(CN)_6 \right]^{3-/4-}$ redox probe decrease, transducing a decrease of charge transfer through the SiW_{11} LBL film. This phenomenon can be due to the increase of the electrostatic repulsion between $\left[Fe(CN)_6 \right]^{3-/4-}$ and the more negatively charged SiW_{11} LBL film.
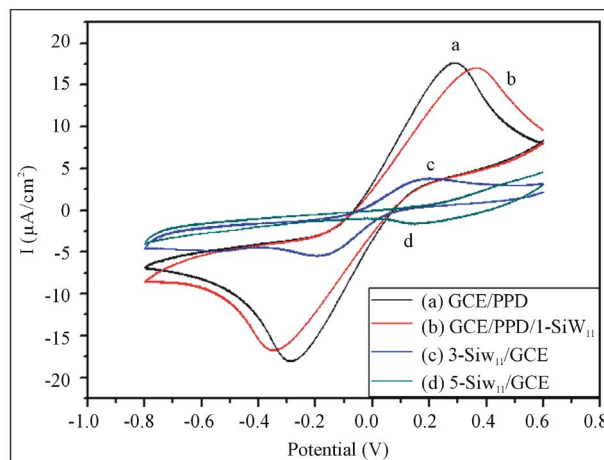

Figure 5. Cyclic voltammograms of $\left[Fe(CN)_6 \right]^{3-/4-}$ **(1 mM, 1 M KCl), at modified electrodes with (PPD/PAH/SiW$_{11}$) n for n = 1, 3 and 5.**

Figure 4 shows a comparison between the cyclic voltammogram of the soluble and immobilized SiW_{11} in LBL films of 5-SiW_{11} layers. Immobilized in LBL film, SiW_{11} displays a close similar electrochemical behavior to that of soluble SiW_{11}. These observations demonstrate that the electrochemical behavior of the SiW_{11} anion is maintained in the multilayer films [40]. Nevertheless, EpcI was shifted to 0.454 V and EpcII to 0.722 V versus Ag/AgCl. The redox peaks were broadened and ΔEpI was found to be around 150 mV whereas $\Delta EpII$ was around 70 mV. The broadening can be related to the large coulombic repulsion between the negative sites of highly-charged polyanions in the same layer, as in [37]. The decrease of reversibility could be attributed to the decrease of charge transfer rate through the poorly conductive PPD layer.

The electrochemical stability of the SiW_{11}/PAH/PPD/GC electrode was investigated in 0.1 M H_2SO_4 solution at a scan rate of 100 mV s^{-1}. After 300 cycles, the cathodic peak current (peak II) still remains about at 93% of the initial value. These results indicate that the SiW_{11}/PAH/polyPPD/GC electrode present a good stability.

3.2.2. SEM Characterization of SiW$_{11}$/polyPPD Film
In order to observe the SiW_{11}/polyPPD film in an accurate way, the film was electrodeposited onto gold electrode, by the method described above. Near the border, we can clearly see that the majority of the electrode surface is covered by the PPD film and there is no appearance of dendrite structure (**Figure 6(a)**), so we can say that the morphologies seen at the polyPPD/gold electrode surface are similar to those at the polyPPD/GC surface. The successful immobilization of SiW_{11} in the electrode surface is confirmed by the energy-dispersive X-ray (ED-X) analyses (**Figure 7**), showing the presence of W and
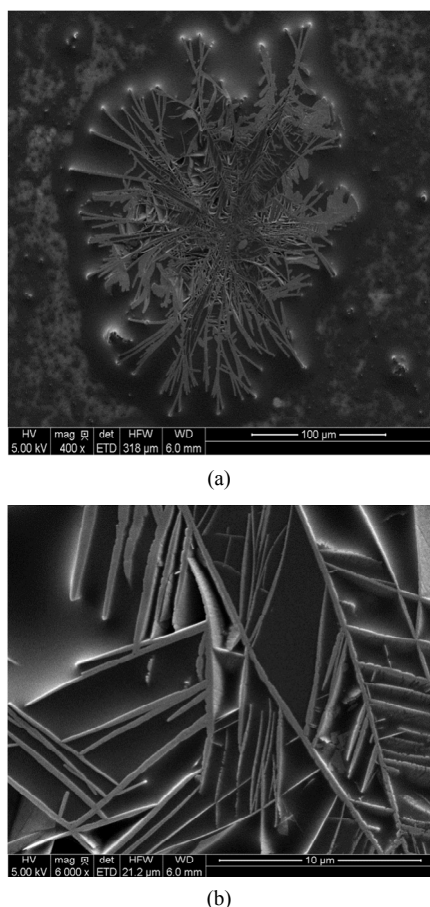
(a)

(b)

Figure 6. (a) PPD/SiW$_{11}$ monolayer film (×400) (WD = Working distance, HFW = High Field View (distance x, y scanned), det LFD = type of used detector is ETD Everhart Thornley (called secondary electron detector = topographic contrast), mag = Magnific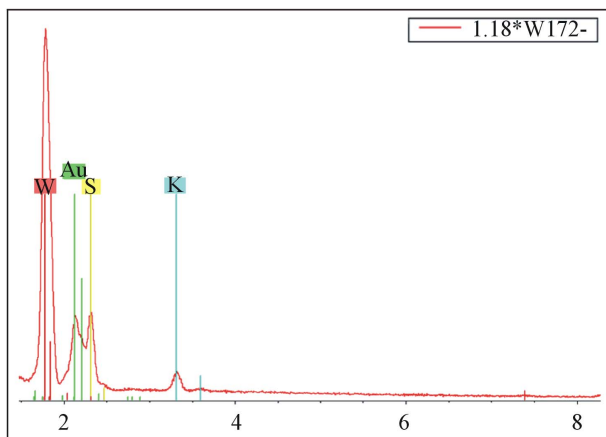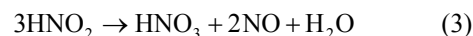ation value to a Polaroid format, HV = accelerating voltage); (b) PPD/SiW$_{11}$ monolayer film (×6000) (WD = Working distance, HFW = High Field View (distance x, y scanned), det LFD = type of used detector is ETD Everhart Thornley (called secondary electron detector = topographic contrast), mag = Magnification value to a Polaroid format, HV = accelerating voltage).

Figure 7. Representative EDX analysis of multilayer films.

O. Several large crystallites and dendrites can be seen (size around 200 μm), especially in the central zone of the electrode, which showed a significantly rough surface.

In this study, amplification of the image obtained at the electrode center revealed the presence of highly populated crystallite regions (**Figure 6(b)**). Besides, the electrode surface appeared as a tri-dimensional structure with a high "apparent" rugosity. The image shows that the product consists of nanometer-sized platelet structures (80 - 300 nm thick) and that some of the nanostructures agglomerate together. The formation of dendrite structure after deposition of SiW$_{11}$ has already been observed in [40].

3.3. Reduction of Nitrite Using GCE/SiW$_{11}$/PAH Multilayer-Modified Electrode

In this acidic solution, most nitrite ions are protonated, the question is which are the actual reactive species, because the pKa of HNO$_2$ is 3.3 [49,50] Equation (3) suggest that the active species could be HNO$_2$ and/or NO. As HNO$_2$ disproportionates in fairly acidic solution, even though the rate of reaction (3) is known to be low [49,50].

$$3HNO_2 \rightarrow HNO_3 + 2NO + H_2O \tag{3}$$

Nitrite might be reduced to NO instantly [51] by reacting with $H_2SiW_{11}O_{39}^{8-}$ and $H_4SiW_{11}O_{39}^{8-}$ as soon as HNO$_2$ arrives at the (GC/PPD/PAH/SiW$_{11}$) films on electrode surface. The resulting $H_2SiW_{11}O_{39}^{8-}$ is then reduced to $H_4SiW_{11}O_{39}^{8-}$ to facilitate the mediation effect for the reduction of nitrite. The electrocatalytic behavior of a SiW$_{11}$ modified electrode towards nitrite can be explained by the following mechanism:
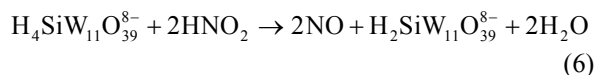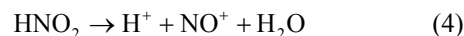
$$HNO_2 \rightarrow H^+ + NO^+ + H_2O \tag{4}$$

$$NO^+ + 1e^- \rightarrow NO \tag{5}$$

$$H_4SiW_{11}O_{39}^{8-} + 2HNO_2 \rightarrow 2NO + H_2SiW_{11}O_{39}^{8-} + 2H_2O \tag{6}$$

Figure 8 shows the behavior of SiW$_{11}$ immobilized in LBL film of 5-SiW$_{11}$ layers in 0.1 M H$_2$SO$_4$ aqueous solution at pH 1.2 containing nitrite in various concentrations (from 0.1 mM to 3.6 mM).

The catalytic effect appears on the reduction peak II of SiW$_{11}$, it increases whereas the corresponding oxidation current decreases. This typical for a reduction process mediated by a reduction catalyst. Equation (6) presents the possible overall process.

We find that the ratios Ipa/Ipc of the second couple are 0.45, 0.51 and 0.6 corresponding to nitrite concentrations of 1, 2 and 2.8 mM respectively, this ratio is increased with stepwise addition of nitrite. No response is observed on the bare GC electrode, in the range of 0.8 to −0.8 V in
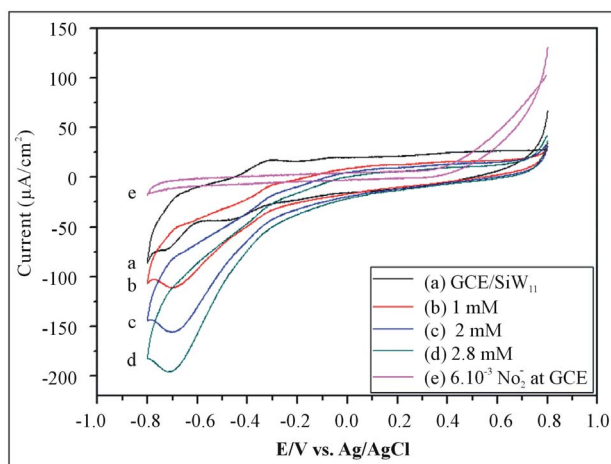
Figure 8. Cyclic voltammograms showing the catalytic activity of SiW$_{11}$/LBL film (5-SiW$_{11}$ layers) at different nitrite concentrations: 0, 1, 2 and 2.8 mmol/L.

0.1 M H$_2$SO$_4$ solutions containing 0.4 mM and 0.6 mM of NO$_2^-$, as shown in (**Figure 8(e)**).

3.4. Effect of the Number of Layers on the Nitrite Reduction

In order to confirm the effect of the number of layers on the electrochemical properties, the electrochemical behaviors of SiW$_{11}$-modified electrode were investigated.

With increasing number of SiW$_{11}$ layers, the catalytic reduction of nitrite increases. For example, the electrocatalytic current observed with 5- SiW$_{11}$ layers is higher than the current observed with 2- SiW$_{11}$ layers in the presence of 0.1 mM of nitrite. The response of the modified electrode toward nitrite is practically constant when number of layers is high than 5 (**Figure 9**).

3.5. Calibration Curve and Reproducibility

The catalytic peak maximum at potential −0.68 V is linearly dependent on the nitrite concentration, in the range 0.1 mM - 3.6 mM, with correlation coefficient of 0.9991, as shown in **Figure 10**. The reproducibility of the nitrite sensor was studied by using three different sensors, the cathodic peak current corresponding to 2.8 mM of nitrite still remains about 93%.

3.6. Life Time

The stability of the nitrite sensor was investigated over a period of 75 days. The sensor was stored under air at room temperature and the current response to 3 mM of nitrite injection in 0.1 M H$_2$SO$_4$ pH 1.2 was checked at regular intervals. No significant change (< 10%) was observed within this period of time. The stability of this sensor can be attributed to the large amount of SiW$_{11}$ which is deposited on the surface of the electrode.
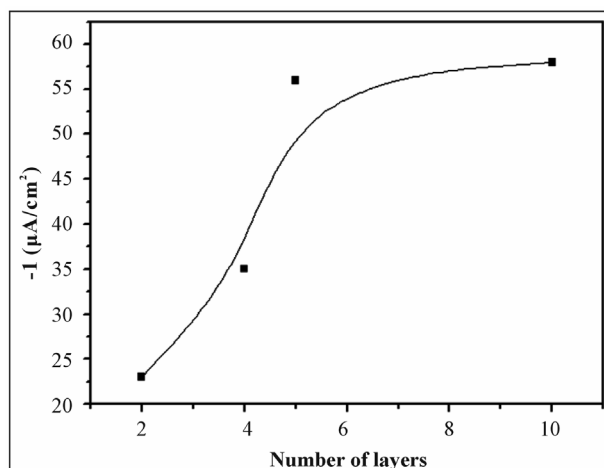

Figure 9. The relationship between peak currents (EpcII) versus number of layers (2 to 10 layers).
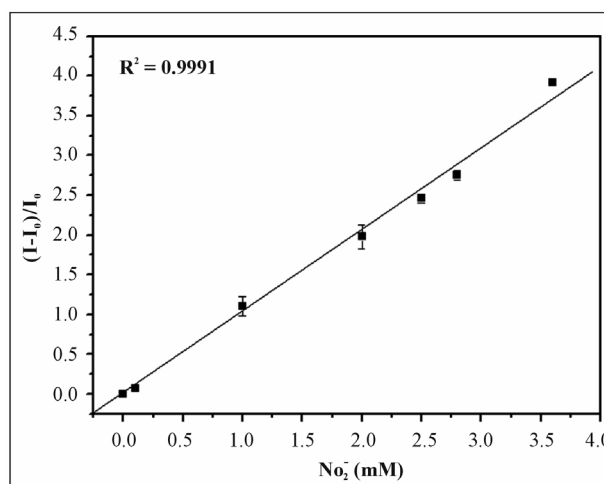

Figure 10. Calibration curve: Linear relationship between the catalytic current and nitrite concentrations at −0.6 V vs. Ag/AgCl. Electrolyte (0.1 M H$_2$SO$_4$), scan rate 100 mV/s.

3.7. Interferences

Our experiments showed that SiW$_{11}$ modified electrode has no catalytic properties towards nitrate molecular (**Figure 2.A.S**). The response of SiW$_{11}$ modified electrode was also tested toward other ions such as phosphate (**Figure 2.B.S**) and perchlorate (**Figure 2.C.S**), with concentrations between 2 mM and 6 mM. No significant increase in the current was observed. Hence, this proves the selective determination of nitrite because it eliminates the major interferences such as nitrate.

4. Conclusions

In this study, we demonstrate that the second redox couple of SiW$_{11}$ anion can act as a mediator for the catalytic reduction of nitrite in aqueous solution with H$_2$SO$_4$ concentration (0.1 M). The electrochemical behavior of the

modified electrode was studied using cyclic voltammetry. Catalytic reduction of nitrite can be employed as a new method for determination of nitrite in real sample such as weak liquor existing in the wood and paper industry. This method is simple, low-cost and precise for routine control and can be carried out directly without any separation or pretreatment due to the selective electrocatalytic reduction of nitrite.

The catalytic reduction peak current showed a linear dependent on the nitrite concentration and a linear calibration curve was obtained. Further studies for using this nitrite sensor in real samples are under investigation.

5. Acknowledgements

REFERENCES

[1] I. A. Wolf and A. E. Wasserman, "Nitrates, Nitrites, and Nitrosamines," *Science*, Vol. 177, No. 4043, 1972, pp. 15-19. doi:10.1126/science.177.4043.15

[2] W. Lijinsky and S. S. Epstein, "Nitrosamines as Environmental Carcinogens," *Nature*, Vol. 225, No. 5227, 1970, pp. 21-23. doi:10.1038/225021a0

[3] A. J. Dunham. R. M. Barkley and R. E. Sievers, "Aqueous Nitrite Ion Determination by Selective Reduction and Gas-Phase Nitric-Oxide Chemiluminescence," *Analytical Chemistry*, Vol. 67, No. 1, 1995, pp. 220-224. doi:10.1021/ac00097a033

[4] V. Y. Titov and Y. M. Petrenko, "Proposed Mechanism of Nitrite-Induced Methemoglobinemia," *Biochemistry* (*Moscow*), Vol. 70, No. 4, 2005, pp. 473-483.

[5] G. M. Greenway, S. J. Haswell and P. H. Petsul, "The Development of an On-Chip Micro-Flow Injection Analysis of Nitrate with a Cadmium Redactor," *Analytica Chimica Acta*, Vol. 387, No. 1, 1999, pp. 1-10. doi:10.1016/S0003-2670(99)00047-1

[6] M. I. H. Helaleh and T. J. Korenaga, "Chromatographic Method for Simultaneous Determination of Nitrate and Nitrite in Human Salivia," *Journal of Chromatography B*: *Biomedical Sciences and Applications*, Vol. 744, No. 2, 2000, pp. 433-437. doi:10.1016/S0378-4347(00)00264-4

[7] W. J. R. Santos, A. L. Sousa, R. C. S. Luz, F. S. Damos, L. T. Kubota, A. A. Tanaka and S. M. C. N. Tanaka, "Amperometric Sensor for Nitrite Using a Glassy Carbon Electrode Modified with Alternating Layers of Iron(III) Tetra-(N-methyl-4-pyridyl)-porphyrin and Cobalt(II) Tetrasulfonated Phthalocyanine," *Talanta*, Vol. 70, No. 3, 2006, pp. 588-594. doi:10.1016/j.talanta.2006.01.023

[8] J. E. Newbry and M. P. L. de Haddad, "Amperometric Determination of Nitrite by Oxidation at a Glassy Carbon Electrode," *Analyst*, Vol. 110, No. 1, 1985, pp. 81-82. doi:10.1039/an9851000081

[9] M. Trojanowiez, W. Matuszewski and B. Szostek, "Simu-

[10] Z. H. Wen and T. F. Kang, "Determination of Nitrite Using Sensors Based on Nickel Phthalocyanine Polymer Modified Electrodes," *Talanta*, Vol. 62, No. 2, 2004, pp. 351-355. doi:10.1016/j.talanta.2003.08.003

[11] P. Tau and T. Nyokong, "Electrocatalytic Activity of Arylthio Tetra-Substituted Oxotitanium(IV) Phthalocyanines towards the Oxidation of Nitrite," *Electrochimica Acta*, Vol. 52, No. 13, 2007, pp. 4547-4553. doi:10.1016/j.electacta.2006.12.059

[12] J. Obirai and T. Nyokong, "Electrochemical and Catalytic Properties of Chromium Tetra Aminophthalocyanine," *Journal of Electroanalytical Chemistry*, Vol. 573, No. 1, 2004, pp. 77-85. doi:10.1016/S0022-0728(04)00341-9

[13] A. Y. Chamsi and A. G. Fogg, "Oxidative Flow Injection Amperometric Determination of Nitrite at an Electrochemically Pre-Treated Glassy Carbon Electrode," *Analyst*, Vol. 113, No. 11, 1988, pp. 1723-1727. doi:10.1039/an9881301723

[14] Z. Zhao and X. Cai, "Determination of Trace Nitrite by Catalytic Polarography in Ferrous Iron Thiocyanate Medium," *Journal of Electroanalytical Chemistry and Interfacial Electrochemistry*, Vol. 252, No. 2, 1988, pp. 361-370. doi:10.1016/0022-0728(88)80222-5

[15] J. N. Barisci and G. G. Wallace, "Detection of Nitrite Using Electrodes Modified with an Electrodeposited Ruthenium-Containing Polymer," *Analytical Letters*, Vol. 24, No. 11, 1991, pp. 2059-2073. doi:10.1080/00032719108053033

[16] S. A. Wring and J. P. Hart, "Chemically Modified, Carbon-Based Electrodes and Their Application as Electrochemical Sensors for the Analysis of Biologically Important Compounds," *Analyst*, Vol. 117, No. 8, 1992, pp. 1215-1229. doi:10.1039/an9921701215

[17] J. A. Cox, M. E. Tess and T. E. Cummings, "Electrochemistry of Organized Monolayers of Thiols and Related Molecules on Electrodes," *Reviews in Analytical Chemistry*, Vol. 15, 1996, pp. 173-223.

[18] J. P. Hart and S. A. Wring, "Recent Developments in the Design and Application of Screen-Printed Electrochemical Sensors for Biomedical, Environmental and Industrial Analyses," *TrAC Trends in Analytical Chemistry*, Vol. 16, No. 2, 1997, pp. 89-103. doi:10.1016/S0165-9936(96)00097-0

[19] J. Wang, P. V. A. Pamidi and C. Parrado, "Sol-Gel-Derived Cobalt Phthalocyanine-Dispersed Carbon Composite Electrodes for Electrocatalysis and Amperometric Flow Detection," *Electroanalysis*, Vol. 9, No. 12, 1997, pp. 908-911. doi:10.1002/elan.1140091208

[20] R. Ojani, J. B. Raoof and E. Zarei, "Electrocatalytic Reduction of Nitrite Using Ferricyanide; Application for Its Simple and Selective Determination," *Electrochimica Acta*, Vol. 52, No. 3, 2006, pp. 753-759. doi:10.1016/j.electacta.2006.06.005

[21] R. Ojani, J. B. Raoof and E. Zarei, "Poly(ortho-toluidine) Modified Carbon Paste Electrode: A Sensor for Electro-

lataneous Determination of Nitrite and Nitrate in Water Using Flow-Injection Biamperometry," *Analytica Chimica Acta*, Vol. 261, No. 1-2, 1992, pp. 391-398. doi:10.1016/0003-2670(92)80218-V

catalytic Reduction of Nitrite," *Electroanalysis*, Vol. 20, No. 4, 2008, pp. 379-385. doi:10.1002/elan.200704045

[22] K. Jiang, H. Zhang, C. Shannon and W. Zhan, "Preparation and Characterization of Polyoxometalate/Protein Ultrathin Films Grown on Electrode Surfaces Using Layer-by-Layer Assembly," *Langmuir*, Vol. 24, No. 7, 2008, pp. 3584-3589. doi:10.1021/la704015j

[23] M. T. Pope, "Heteropoly and Isopoly Oxometalates," Springer Verlag, New York, 1983, pp. 23-27. doi:10.1007/978-3-662-12004-0

[24] M. T. Pope, In: G. Wilkinson, R. D. Gillard and J. A. McCleverty, Eds., *Comprehensive Coordination Chemistry*, Pergamon Press, 1987, Vol. 3, pp 1023.

[25] L. C. W. Baker and D. C. Glick, "Present General Status of Understanding of Heteropoly Electrolytes and a Tracing of Some Major Highlights in the History of Their Elucidation," *Chemical Reviews*, Vol. 98, No. 1, 1998, pp. 3-50. doi:10.1021/cr960392l

[26] C. L. Hill, "Polyoxometalates," *Chemical Reviews*, Vol. 98, No. 1, 1998, pp. 1-2. doi:10.1021/cr960395y

[27] M. Sadakane and E. Steckhan, "Electrochemistry and Electrocatalysis of Polyoxometalates," *Chemical Reviews*, Vol. 98, No. 1, 1998, pp. 219-237. doi:10.1021/cr960403a

[28] C. L. Hill and C. M. Prosser-McCartha, "Homogeneous Catalysis by Transition Metal Oxygen Anion Clusters," *Coordination Chemistry Reviews*, Vol. 143, 1995, pp. 407-455. doi:10.1016/0010-8545(95)01141-B

[29] B. Keita and L. Nadjo, "Polyoxometalate-Based Homogeneous Catalysis of Electrode Reactions: Recent Achievements," *Journal of Molecular Catalysis A*: *Chemical*, Vol. 262, No. 1-2, 2007, pp. 190-215. doi:10.1016/j.molcata.2006.08.066

[30] R. Neumann, "Chapter 8," In J. E. Backvall, Ed., *Modern Oxidation Methods*, Wiley-VCH, Weinheim, 2004, pp. 223-251.

[31] J. F. Keggin, "Structure of the Crystals of 12-Phosphotungstic Acid," *Nature*, Vol. 132, 1933, pp. 351-351. doi:10.1038/132351a0

[32] J. F. Keggin, "The Structure and Formula of 12-Phosphotungstic Acid," *Proceedings of the Royal Society London*, *Series A*, Vol. 144, No. 851, 1934, pp. 75-100.

[33] B. Keita, A. Belhouari, L. Nadjo and R. Contant, "Electrocatalysis by Polyoxometalate/Vbpolymer Systems: Reduction of Nitrite and Nitric Oxide," *Journal of Electroanalytical Chemistry*, Vol. 381, No. 1-2, 1995, pp. 243-250. doi:10.1016/0022-0728(94)03710-K

[34] U. Kortz, N. K. Al-Kassem, M. G. Savelieff, N. A. Al Kadi and M. Sadakane, "Synthesis and Characterization of Copper, Zinc, Manganese, and Cobalt-Substituted Dimeric Heteropolyanions, $[(\alpha\text{-}XW_9O_{33})_2M_3(H_2O)_3]^{n-}$ (n = 12, X = AsIII, SbIII, M = Cu^{2+}, Zn^{2+}; n = 10, X = SeIV, TeIV, M = Cu^{2+}) and $[(\alpha AsW_9O_{33})_2WO(H_2O)M_2 (H_2O)_2]^{10-}$ (M = Zn^{2+}, Mn^{2+}, Co^{2+}),", *Inorganic Chemistry*, Vol. 40, No. 18, 2001, pp. 4742-4749. doi:10.1021/ic0101477

[35] G. Decher and J. B. Schenoff, "Multilayer Thin Films," Wiley VCH, Weinheim, 2003, 524p.

[36] Y. Wang, C. Guo, Y. Chen, C. Hu and W. Yu, "Self-Assembled Multilayer Films Based on a Keggin-Type Polyoxometalate and Polyaniline," *Journal of Colloid and Interface Science*, Vol. 264, No. 1, 2003, pp. 176-183. doi:10.1016/S0021-9797(03)00392-8

[37] Y. Feng, Z. Han, J. Peng, J. Lu, B. Xue, L. Li, H. Ma and E. Wang, "Fabrication and Characterization of Multilayer Films Based on Keggin-Type Polyoxometalate and Chitosan," *Materials Letters*, Vol. 60, No. 13-14, 2006, pp. 1588-1593. doi:10.1016/j.matlet.2005.11.069

[38] S. Li, E. Wang, C. Tian, B. Mao, Y. Song, C. Wang and L. Xu, "*In Situ* Fabrication of Amino Acid-Polyoxometalate Nanoparticle Functionalized Ultrathin Films and Relevant Electrochemical Property Study," *Materials Research Bulletin*, Vol. 43, No. 11, 2008, pp. 2880-2886. doi:10.1016/j.materresbull.2007.12.012

[39] D. M. Fernandes, H. M. Carapuça, C. M. A. Brett and A. M. V. Cavaleiro, "Electrochemical Behaviour of Self-Assembly Multilayer Films Based on Iron-Substituted α-Keggin Polyoxotungstates," *Thin Solid Films*, Vol. 518, No. 21, 2010, pp. 5881-5888. doi:10.1016/j.tsf.2010.05.065

[40] D. M. Fernandes, S. M. N. Simoes, H. M. Carapuca and A. M. V. Cavaleiro, "Functionalisation of Glassy Carbon Electrodes with Deposited Tetrabutylammonium Microcrystalline Salts of Lacunary and Metal-Substituted α-Keggin-Polyoxosilicotungstates," *Electrochimica Acta*, Vol. 53, No. 22, 2008, pp. 6580-6588. doi:10.1016/j.electacta.2008.04.071

[41] A. Téazéa, G. Hervéa, R. G. Finke and D. K. Lyon, "α-, β-, and γ-Dodecatungstosilicic Acids: Isomers and Related Lacunary Compounds," In: *Inorganic Syntheses*, John Wiley & Sons, New York, 1990, pp. 85-96. doi:10.1002/9780470132586.ch16

[42] D. U. Jinyan, L. V. Guiqin, H. U. Changwen and W. U. Huaqiang, "Layer-by-Layer Assembly of Silicotungstate Multilayer Films Modified on Glassy Carbon Electrode and Their Electrochemical Behaviors," *Annali di Chimica*, Vol. 97, No. 5-6, 2007, pp. 313-320. doi:10.1002/adic.200790017

[43] L. Cheng, H. Seen, J. Liu and S. Dong, "Electrochemical Behavior of a Series of Undecatungstozincates Monosubstituted by First-Row Transition Metals, $ZnW_{11}M(H_2O) O_{39}{}^{n-}$ (M = Cr, Mn, Fe, Co, Ni, Cu or Zn)," *Journal of the Chemical Society*, *Dalton Transactions*, No. 15, 1999, pp. 2619-2626. doi:10.1039/a901846h

[44] C. Rocchiccioli-Deltcheff, M. Fournier, R. Franck and R. Thouvenot, "Vibrational Investigations of Polyoxometalates. 2. Evidence for Anion-Anion Interactions in Molybdenum(VI) and Tungsten(VI) Compounds Related to the Keggin Structure," *Inorganic Chemistry*, Vol. 22, No. 2, 1983, pp. 207-216. doi:10.1021/ic00144a006

[45] D. M. Fernandes, C. M. A. Brett and A. M. V. Cavaleiro, "Layer-By-Layer Self-Assembly And Electrocatalytic Properties Of Poly(Ethylenimine)-Silicotungstate Multilayer Composite Films," *Journal of Solid State Electrochemistry*, Vol. 15, No. 4, 2011, pp. 811-819. doi:10.1007/s10008-010-1154-1

[46] I. M. Mbomekalle, B. Keita, Y. W. Lu, L. Nadjo, R. Can-

tant, N. Belai and M. T. Pope, "Synthesis and Electrochemistry of the Monolacunary Dawson-Type Tungstoarsenate $[H_4AsW_{17}O_{61}]^{11-}$ and Some First-Row Transition-Metal Ion Derivatives," *European Journal of Inorganic Chemistry*, Vol. 2004, No. 20, 2004, pp. 4132-4139. doi:10.1002/ejic.200400186

[47] S. D. Chambers, M. T. McDermott and C. A. Lucy, "Covalently Modified Graphitic Carbon-Based Stationary Phases for Anion Chromatography," *Analyst*, Vol. 134, No. 11, 2009, pp. 2273-2280. doi:10.1039/b911988d

[48] J. Liu, L. Cheng, B. Liu and S. Dong, "Covalent Modification of a Glassy Carbon Surface by 4-Aminobenzoic Acid and Its Application in Fabrication of a Polyoxometalates-Consisting Monolayer and Multilayer Films," *Langmuir*, Vol. 16, No. 19, 2000, pp. 7471-7476. doi:10.1021/la9913506

[49] B. Keita, F. Girard, L. Nadjo, R. Contant, R. Belghiche and M. Abbessi, "Cyclic Voltammetric Evidence of Facilitation of the Reduction of Nitrite by the Presence of Molybdenum in Fe- or Cu-Substituted Heteropolytungstates," *Journal of Electroanalytical Chemistry*, Vol. 508, No. 1-2, 2001, pp. 70-80. doi:10.1016/S0022-0728(01)00516-2

[50] S. Dong, X. Xi and M. Tian, "Study of the Electrocatalytic Reduction of Nitrite with Silicotungstic Heteropolyanion," *Journal of Electroanalytical Chemistry*, Vol. 385, No. 2, 1995, pp. 227-233. doi:10.1016/0022-0728(94)03770-4

[51] L. Ruhlmann and G. Genet, "Wells-Dawson-Derived Tetrameric Complexes $\{K_{28}H_8[P_2W_{15}Ti_3O60.5]4\}$ Electrochemical Behaviour and Electrocatalytic Reduction of Nitrite and of Nitric Oxide," *Journal of Electroanalytical Chemistry*, Vol. 568, 2004, pp. 315-321. doi:10.1016/j.jelechem.2004.02.020
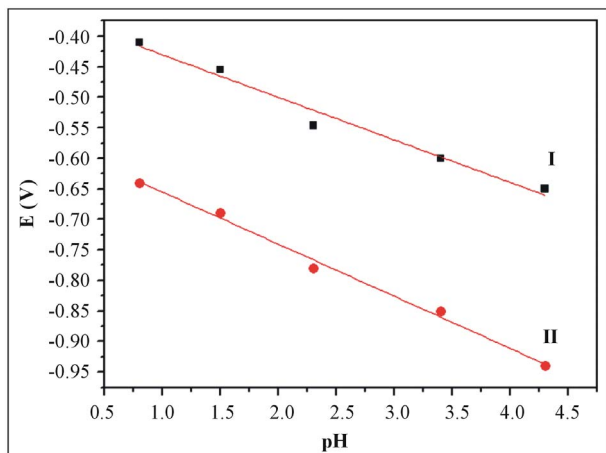
Appendix

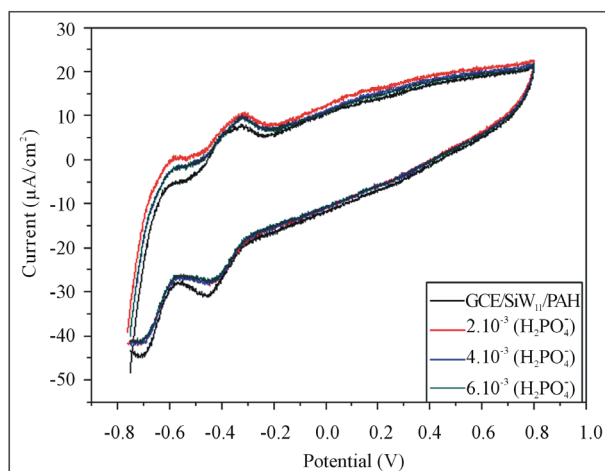**Figure 1S. The relationship between cathodic potentials of two redox waves (EpcI and EpcII) and pH.**

Figure 2.B.S. Cyclic voltammograms of the SiW$_{11}$/LBL/GC electrode in 0.1 M H$_2$SO$_4$ solution containing (a) 0 mM, (b) 2 mM, (c) 4 mM and (d) 6 mM HPO$_4^-$. Scan rate: 100 mV/s.
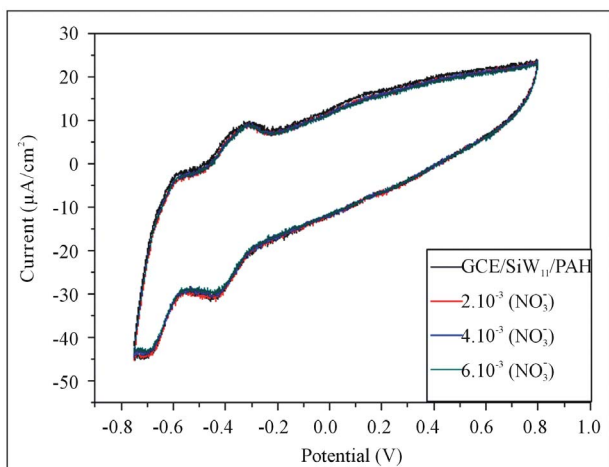

Figure 2.A.S. Cyclic voltammograms of the SiW$_{11}$/LBL/GC electrode in 0.1 M H$_2$SO$_4$ solution containing (a) 0 mM, (b) 2 mM, (c) 4 mM and (d) 6 mM NO$_3^-$. Scan rate: 100 mV/s.
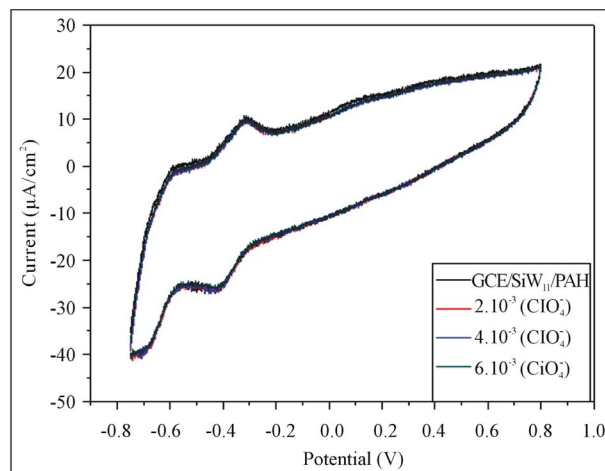

Figure 2.C.S. Cyclic voltammograms of the SiW$_{11}$/LBL/GC electrode in 0.1 M H$_2$SO$_4$ solution containing (a) 0 mM, (b) 2 mM, (c) 4 mM and (d) 6 mM ClO$_4$. Scan rate: 100 mV/s.